

On cascade of kinetic energy in compressible hydrodynamic turbulence

Petr Hellinger^{1,2†}, Andrea Verdini^{3,4}, Simone Landi^{3,4}, Luca Franci^{5,4}, Emanuele Papini^{3,4}, and Lorenzo Matteini⁶

¹Astronomical Institute, CAS, Prague, Czech Republic

²Institute of Atmospheric Physics, CAS, Prague, Czech Republic

³Università di Firenze, Italy

⁴INAF, Osservatorio Astrofisico di Arcetri, Firenze, Italy

⁵Queen Mary University of London, UK

⁶Imperial College, London, UK

(Received xx; revised xx; accepted xx)

Properties of the turbulent cascade of kinetic energy are studied using direct numerical simulations of three-dimensional hydrodynamic decaying turbulence with a moderate Reynolds number and the initial Mach number $M = 1$. Compressible and incompressible versions of the Kármán-Howarth-Monin (KHM) and low-pass filtering/coarse-graining approaches are compared. In the simulation the total energy is well conserved; the scale dependent KHM and coarse-grained energy equations are also well conserved; the two approaches show similar results, the system does not have an inertial range for the cascade of kinetic energy, the region where this cascade dominates also have a non-negligible contribution of the kinetic-energy decay, dissipation, and pressure-dilatation effects. While the two approaches give semi-quantitatively similar results for the kinetic energy cascade, dissipation and pressure-dilatation rates, they differ in the increment separation and filtering scales; these scales are not simply related. The two approaches may be used to find the inertial range and to determine the cascade/dissipation rate of the kinetic energy.

Key words:

1. Introduction

Turbulence in compressible fluids is not well understood. One of the open questions is the existence of the so called inertial range, where the kinetic energy cascades (usually from large to small scales) without any losses. In the incompressible approximation hydrodynamic (HD) turbulence typically exhibits such inertial range provided that a large separation exists between the driving/energy containing scales and the dissipation ones. These properties are well described by the Kármán-Howarth-Monin (KHM) equation (de Karman & Howarth 1938; Monin & Yaglom 1975) for statistically homogeneous turbulence. This equation represents a scale-dependent energy conservation and relates the driving/decay of kinetic energy, its cascade and dissipation. The inertial range can be formally defined as the region where the driving/decay and dissipation are negligible and

† Email address for correspondence: petr.hellinger@asu.cas.cz

so that the dominant process is the cascade; this leads in the infinite Reynolds number limit to so called exact (scaling) laws for isotropic media (Kolmogorov 1941; Frisch 1995).

In the case of compressible HD turbulence, the kinetic energy and the internal energy are coupled via the dissipation as well as through compressible (pressure dilatation) effects. In this case it is not clear if there can be an inertial range of the kinetic energy. One may consider the total (kinetic+internal) energy, that is strictly conserved, but it is unclear if there is a cascade of the total energy (cf., Eyink & Drivas 2018). Galtier & Banerjee (2011) derived the KHM equation for the total (kinetic and internal) energy assuming that the internal energy is governed by the isothermal closure. This closure, however, partly decouples the internal and kinetic energies and does not conserve the total energy. It is unclear if all or only a part of pressure dilatation effects are present in such a system. The cascade of the kinetic energy and pressure dilatation effects have not yet been studied in detail within the KHM approach. On the other hand, the filtering/coarse graining approach (Germano 1992; Eyink & Aluie 2009) has been applied to the compressible turbulence (Aluie 2011, 2013) to derive relations equivalent to the KHM equation. In particular, Aluie *et al.* (2012) show that the energy exchanges between the kinetic and internal energies appear (at least for some parameters) on large scales and that there may exist a range of scales where the kinetic energy cascades in a conservative way, forming an inertial range similar to that in the incompressible HD approximation. Here we reexamine the KHM equation for the cascade of kinetic energy in compressible HD following Galtier & Banerjee (2011), we test it on results of numerical simulations and compare these results with the coarse-graining approach. The paper is organized as follows: in section 2 we present an overview of the direct 3D HD simulation with the initial Mach number $M = 1$. In section 3 we present the KHM equation for the kinetic energy for incompressible and compressible HD and we test these two versions of KHM equation on the results of the simulation. In section 4 we compare these results with the coarse-graining approach assuming both incompressible and compressible approximations. Finally, in section 5 we discuss the results.

2. Numerical simulation

Here we use a 3D pseudo-spectral compressible hydrodynamic code derived from the compressible MHD code (Verdini *et al.* 2015) based on P3DFFT library (Pekurovsky 2012) and FFTW3 (Frigo & Johnson 2005). The code resolves the compressible Navier-Stokes equations, for the fluid density ρ , velocity \mathbf{u} , and the pressure p :

$$\frac{\partial \rho}{\partial t} + \nabla \cdot (\rho \mathbf{u}) = 0, \quad (2.1)$$

$$\frac{\partial(\rho \mathbf{u})}{\partial t} + \nabla \cdot (\rho \mathbf{u} \mathbf{u}) = -\nabla p + \nabla \cdot \boldsymbol{\tau}, \quad (2.2)$$

completed with an equation for the temperature $T = p/\rho$

$$\frac{\partial T}{\partial t} + (\mathbf{u} \cdot \nabla)T = \alpha \Delta T + (\gamma - 1) \left(-T \nabla \cdot \mathbf{u} + \frac{1}{\rho} \nabla \mathbf{u} : \boldsymbol{\tau} \right) \quad (2.3)$$

where $\boldsymbol{\tau}$ is the viscous stress tensor ($\tau_{ij} = \mu (\partial u_i / \partial x_j + \partial u_j / \partial x_i - 2/3 \delta_{ij} \partial u_k / \partial x_k)$; here the dynamic viscosity μ is assumed to be constant) and α is the thermal diffusivity (we set $\alpha = \mu$ and $\gamma = 5/3$); the colon operator denotes the double contraction of second order tensors, $\mathbf{A} : \mathbf{B} = \sum_{ij} A_{ij} B_{ij}$. The box size is $(2\pi)^3$ (with a grid of 1024^3 points), periodic boundary conditions are assumed. The simulation is initialized with isotropic, random-phase, solenoidal fluctuations ($\nabla \cdot \mathbf{u} = 0$) on large scales (with wave vectors

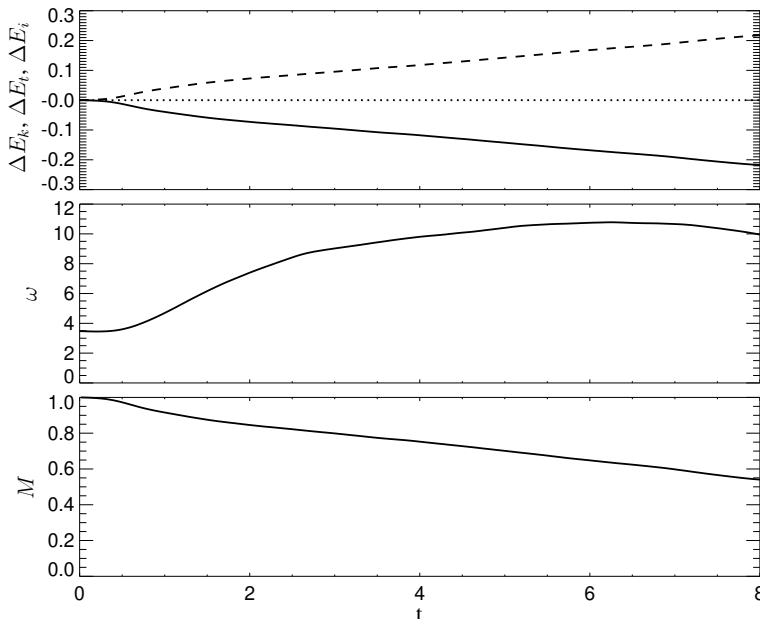


FIGURE 1. Evolution of (top) the relative changes in the kinetic energy ΔE_k (solid line), the total energy ΔE_t (dotted line), and the internal energy ΔE_i (dashed), (middle) vorticity ω , (bottom) Mach number M as functions of time.

$k = |\mathbf{k}| \leq 4$) having the rms Mach number $M = 1$ and a k^{-1} 1-D power spectrum profile. We set the (constant) dynamic viscosity $\mu = 2.8 \cdot 10^{-3}$.

The evolution of the simulation is shown in Figure 1. In the simulation the total energy $E_t = E_k + E_i$ is well conserved. Here $E_k = \langle \rho u^2 \rangle / 2$ is the kinetic energy and $E_i = \langle \rho T \rangle / (\gamma - 1)$ is the internal one (here $\langle \bullet \rangle$ denotes averaging over the simulation box). Top panel of Figure 1 displays the evolution of the relative changes in these energies, $\Delta E_{k,i,t} = (E_{k,i,t}(t) - E_{k,i,t}(0)) / E_t(0)$. The relative decrease of the total energy is negligible, $\Delta E_t(t = 8) \sim -4 \cdot 10^{-6}$. The middle panel of Figure 1 shows the evolution of the rms of the vorticity $\boldsymbol{\omega} = \nabla \times \mathbf{u}$. The vorticity reaches a maximum at $t \simeq 6.2$; this is a signature of a fully developed turbulent cascade. The bottom panel of Figure 1 displays the evolution of the average Mach number M (i.e., the ratio between rms of the velocity and the mean sound speed). M slowly decreases during the evolution due to the decay of the level of fluctuations as well as due to the turbulent heating that leads to an increasing sound speed.

Figure 2 shows the power spectral density (PSD) of the velocity fluctuation at the time 6.3, around the maximum activity of the vorticity, when turbulence is expected to be fully developed. The PSD does not exhibit a clear, Kolmogorov like spectrum, thus suggesting that there is no inertial range in the simulation. This is likely due to the small system size (small Reynolds number) and/or due to the compressible effects. In the following sections we'll quantify these effects using KHM and coarse graining approaches.

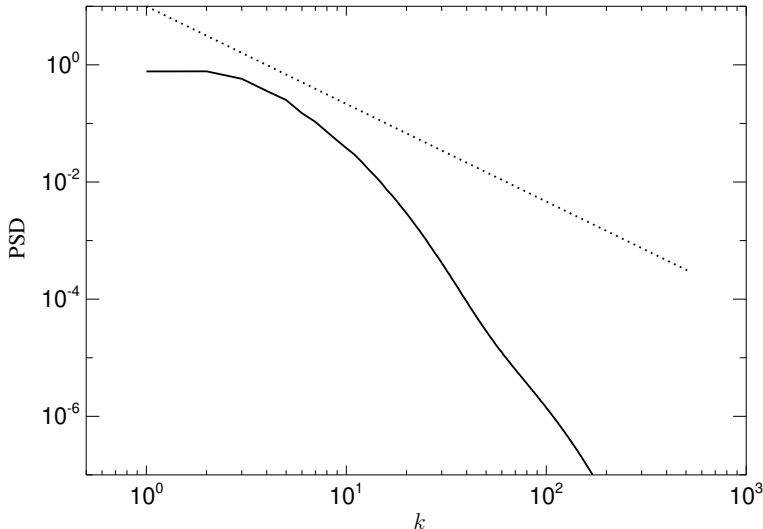


FIGURE 2. Power spectral density of \mathbf{u} as a function of the wave vector k . The dotted line denotes a dependence $\propto k^{-5/3}$.

3. KHM equation

3.1. Incompressible HD

For the incompressible Navier-Stokes equation

$$\frac{\partial \mathbf{u}}{\partial t} + \nabla \cdot (\mathbf{u}\mathbf{u}) = -\frac{\nabla p}{\rho} + \nu \Delta \mathbf{u}, \quad (3.1)$$

where \mathbf{u} is the velocity field, ρ the density, p the pressure, ν is the kinematic viscosity. For statistically homogeneous decaying turbulence one can get from Equation (3.1) the following form of the KHM equation (de Karman & Howarth 1938; Monin & Yaglom 1975) in the terms of structure functions of the increments of the velocity field $\delta \mathbf{u} = \mathbf{u}(\mathbf{x} + \mathbf{l}) - \mathbf{u}(\mathbf{x})$

$$\frac{\partial S^{(i)}}{\partial t} + \nabla_{\mathbf{l}} \cdot \mathbf{Y}^{(i)} = 2\nu \Delta_{\mathbf{l}} S^{(i)} - 4\epsilon, \quad (3.2)$$

where $S^{(i)} = \langle |\delta \mathbf{u}|^2 \rangle$, $\mathbf{Y}^{(i)} = \langle \delta \mathbf{u} |\delta \mathbf{u}|^2 \rangle$ and $\langle \bullet \rangle$ denotes statistical/spatial averaging ($S^{(i)}$ and $\mathbf{Y}^{(i)}$ are functions of \mathbf{l}). Equation (3.2) is simply related to the original form of the KHM equation that involves the cross-correlation $\langle \mathbf{u}(\mathbf{x} + \mathbf{l}) \cdot \mathbf{u}(\mathbf{x}) \rangle$ (cf., Frisch 1995)

$$2 \frac{\partial}{\partial t} \langle \mathbf{u}(\mathbf{x} + \mathbf{l}) \cdot \mathbf{u}(\mathbf{x}) \rangle - \nabla_{\mathbf{l}} \cdot \mathbf{Y}^{(i)} = 4\nu \Delta_{\mathbf{l}} \langle \mathbf{u}(\mathbf{x}) \cdot \mathbf{u}(\mathbf{x} + \mathbf{l}) \rangle \quad (3.3)$$

since $S^{(i)} = 2\langle |\mathbf{u}|^2 \rangle - 2\langle \mathbf{u}(\mathbf{x} + \mathbf{l}) \cdot \mathbf{u}(\mathbf{x}) \rangle$ and $\partial \langle |\mathbf{u}|^2 \rangle / \partial t = -2\epsilon$. Note that here the superscript (i) denotes the incompressible approximation. Equation (3.2) represents a scale-dependent energy-like conservation and relates the decay of kinetic energy $\partial S^{(i)} / \partial t$, the (incompressible) dissipation rate (per mass)

$$\epsilon = \nu \langle \nabla \mathbf{u} : \nabla \mathbf{u} \rangle, \quad (3.4)$$

the cascade rate $\nabla_{\mathbf{l}} \cdot \mathbf{Y}^{(i)}$, and the dissipation term $\nu \Delta_{\mathbf{l}} \langle |\delta \mathbf{u}|^2 \rangle$. The inertial range can be formally defined as the region where the decay and dissipation terms are negligible so that

$$\nabla_{\mathbf{l}} \cdot \mathbf{Y}^{(i)} = -4\epsilon. \quad (3.5)$$

For isotropic media, in the infinite Reynolds number limit, Equation (3.5) leads to the exact (scaling) laws (Kolmogorov 1941; Frisch 1995). Equation (3.2) is more general and may be directly tested in numerical simulations (e.g., Gotoh *et al.* 2002) since large Reynolds numbers needed for existence of the inertial range are computationally challenging (cf., Ishihara *et al.* 2009).

3.2. Compressible HD

Here we assume compressible Navier-Stokes equations, Equations (2.1,2.2), and investigate the structure function $S = \langle \delta \mathbf{u} \cdot \delta(\rho \mathbf{u}) \rangle$ assuming a statistically homogeneous system following Galtier & Banerjee (2011). After some manipulations (see appendix A for details) we get

$$\frac{\partial S}{\partial t} + \nabla_{\mathbf{l}} \cdot \mathbf{Y} + R = C_p - C_\tau + 2 \langle \delta p \delta \theta \rangle - 2 \langle \delta \boldsymbol{\tau} : \delta \boldsymbol{\Sigma} \rangle, \quad (3.6)$$

where $\mathbf{Y} = \langle \delta \mathbf{u} [\delta(\rho \mathbf{u}) \cdot \delta \mathbf{u}] \rangle$, is a third-order structure function, $\theta = \nabla \cdot \mathbf{u}$ is the dilatation, $\boldsymbol{\Sigma} = \nabla \mathbf{u}$ is the strain tensor, and $R = \langle \delta \mathbf{u} \cdot (\theta' \rho \mathbf{u} - \theta \rho' \mathbf{u}') \rangle$.

Here C_p and C_τ are ‘correction’ terms to $\langle \delta p \delta \theta \rangle$ and $\langle \delta \boldsymbol{\tau} : \delta \boldsymbol{\Sigma} \rangle$, respectively,

$$C_p = \mathcal{C}[\mathbf{u}, \nabla p] \quad C_\tau = \mathcal{C}[\mathbf{u}, \nabla \cdot \boldsymbol{\tau}], \quad (3.7)$$

where

$$\mathcal{C}[\mathbf{a}, \mathbf{b}] = \left\langle \delta \mathbf{a} \cdot \delta \mathbf{b} - \delta(\rho \mathbf{a}) \cdot \delta \left(\frac{\mathbf{b}}{\rho} \right) \right\rangle = \left(\frac{\rho'}{\rho} - 1 \right) \mathbf{a}' \cdot \mathbf{b} + \left(\frac{\rho}{\rho'} - 1 \right) \mathbf{a} \cdot \mathbf{b}'.$$

The C_p and C_τ terms depend on the level of density fluctuations in the system.

The two terms, S and \mathbf{Y} , are natural compressible generalization of $S^{(i)}$ and $\mathbf{Y}^{(i)}$, respectively. The R term presents an additional compressible energy-transfer channel (cf., Galtier & Banerjee 2011); we do not see an obvious way how to turn this term to a divergence form similar to $\nabla_{\mathbf{l}} \cdot \mathbf{Y}$. The term $\langle \delta p \delta \theta \rangle$ is a structure-function formulation of the pressure dilation effect $p\theta$. The viscous term $\langle \delta \boldsymbol{\tau} : \delta \boldsymbol{\Sigma} \rangle$ corresponds to a combination of the two dissipation terms in the incompressible case $2\epsilon - \nu \Delta S^{(i)}$ in Equation (3.2). On large scales, $|\delta \mathbf{x}| \rightarrow \infty$, where the correlations $\langle \boldsymbol{\tau}(\mathbf{x}') : \boldsymbol{\Sigma} \rangle \rightarrow 0$ the viscous term becomes twice the viscous heating rate Q_μ ,

$$\langle \delta \boldsymbol{\tau} : \delta \boldsymbol{\Sigma} \rangle \rightarrow 2 \langle \boldsymbol{\tau} : \boldsymbol{\Sigma} \rangle = 2Q_\mu. \quad (3.8)$$

Equation (3.6) is analogous to Equation (10) of Galtier & Banerjee (2011) but it does not include the isothermal internal energy assumed there (i.e., $p = c_s^2 \rho$, $e = c_s^2 \ln \rho / \rho_0$, c_s : sound speed; see also appendix B). Also, in contrast with Galtier & Banerjee (2011), we do not consider forcing since we investigate decaying turbulence here. Now we can test Equation (3.6) using the simulation results of section 2. We define the departure from zero of this equation as

$$O(l) = \frac{1}{4} \left(-\frac{\partial S}{\partial t} - \nabla_{\mathbf{l}} \cdot \mathbf{Y} - R + 2 \langle \delta p \delta \theta \rangle + C_p - 2 \langle \delta \boldsymbol{\tau} : \delta \boldsymbol{\Sigma} \rangle - C_\tau \right). \quad (3.9)$$

Figure 3 shows (black) the departure O as a function of the scale l (isotropized/averaged over spherical angles) along with the different contributions, the decaying term (blue) $-\partial S / \partial t / 4$, the cascade term (green) $-\nabla_{\mathbf{l}} \cdot \mathbf{Y} / 4 - R / 4$, the pressure dilation term (orange) $\langle \delta p \delta \theta \rangle / 2 + C_p / 4$, and the scale-dependent dissipation term $-\langle \delta \boldsymbol{\tau} : \delta \boldsymbol{\Sigma} \rangle / 2 - C_\tau$. This calculation is done for times 6.2 and 6.3 (see Figure 1) over a reduced box 512^3 (taking every second point in all directions); the structure functions are calculated over the

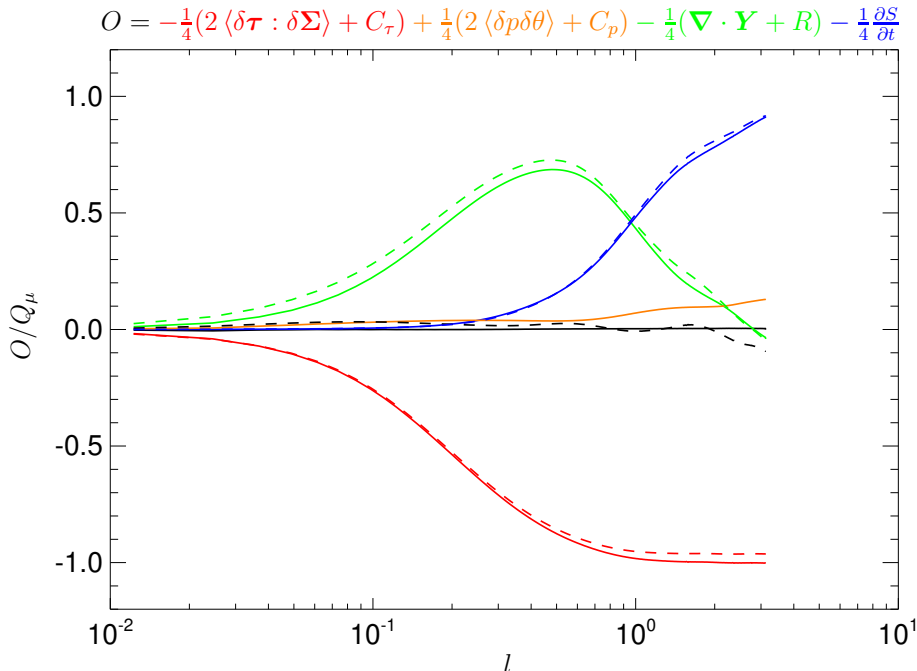


FIGURE 3. (black) The departure O (given by Equation (3.9)) as a function of the scale l along with the different contributions, the decaying term (blue) $-\partial S/\partial t/4$, the cascade term (green) $-\nabla_l \cdot \mathbf{Y}/4 - R/4$, the compressible coupling term (orange) $\langle \delta p \delta \theta \rangle/2 + C_p/4$, and (red) the scale-dependent dissipation term $-\langle \delta \boldsymbol{\tau} : \delta \boldsymbol{\Sigma} \rangle/2 - C_\tau$. Dashed lines show the incompressible equivalent, (black) the departure $O^{(i)}$ (given by Equation (3.9)), the decaying term (blue) $-\rho_0 \partial S^{(i)}/\partial t/4$, the cascade term (green) $-\rho_0 \nabla_l \cdot \mathbf{Y}^{(i)}/4$, and (red) the dissipation term $\rho_0 \nu \Delta S^{(i)}/2 - \rho_0 \epsilon$. O , $O^{(i)}$ and all their contributions are normalized to Q_μ .

full separation space and isotropized/averaged over the spherical angles; the partial time difference is approximated by the finite difference between the two times. Figure 3 demonstrates that the departure O is small as predicted by Equation (3.6); quantitatively we get $|O|/Q_\mu < 0.006$.

The decay, dissipation, and pressure dilatation terms approach zero as $l \rightarrow 0$ and reach their maximum absolute values on large scales: the compressible dissipation term $\langle \delta \boldsymbol{\tau} : \delta \boldsymbol{\Sigma} \rangle/2 \rightarrow Q_\mu$ as expected, and, similarly, $\partial S/\partial t/4 \sim \partial \langle \rho |\mathbf{u}|^2 \rangle / \partial t/2 \simeq 0.91 Q_\mu$ and $\langle \delta p \delta \theta \rangle/2 \sim \langle p \theta \rangle \simeq 0.12 Q_\mu$. On large scales we recover the energy conservation $\partial \langle \rho |\mathbf{u}|^2 \rangle / \partial t/2 = -Q_\mu + \langle p \theta \rangle$; the small error is likely due to the estimation of the time derivative by the finite difference and other numerical effects. The correction terms are small but not negligible $|C_p|/Q_\mu/4 < 0.06$ and $|C_\tau|/Q_\mu/4 < 0.02$ and tend to zero on small and large scales.

The cascade term is important on medium scales but there is no true inertial range since the decay, dissipation as well as the pressure dilatation term are not negligible there. For larger Reynolds numbers one may expect that the decay and pressure dilatation terms become negligible on medium scales and that there is a range of scales the cascade term is compensated by the constant dissipation term

$$\nabla_l \cdot \mathbf{Y} + R = -4Q_\mu, \quad (3.10)$$

i.e., the inertial range.

Figure 3 also displays by dashed lines results of the corresponding incompressible

version of KHM equation, the departure from zero (renormalized by the background density ρ_0) given by

$$O^{(i)}(l) = \frac{\rho_0}{4} \left(-\frac{\partial S^{(i)}}{\partial t} - \nabla_{\mathbf{l}} \cdot \mathbf{Y}^{(i)} + 2\nu \Delta S^{(i)} - 4\epsilon \right), \quad (3.11)$$

The incompressible terms are comparable to their compressible counterparts. In particular, the dissipation terms are close to each other. This indicates that most of the dissipation is incompressible. On the other hand, $\rho_0 \nabla_{\mathbf{l}} \cdot \mathbf{Y}^{(i)}$ and $\nabla_{\mathbf{l}} \cdot \mathbf{Y}$ are almost identical, the decrease of the cascade rate in the compressible KHM is due to the compressible R term.

4. Coarse-graining approach

Let us now compare the structure function approach with the coarse graining one. This method is based on scale-dependent filtering of the compressible Navier-Stokes equation (cf., Aluie 2013). For any field $a(\mathbf{x})$ one defines a coarse-grained (low-pass filtered) field

$$\bar{a}_\ell(\mathbf{x}) = \int_V G_\ell(\mathbf{r}) a(\mathbf{x} + \mathbf{r}) d^3 \mathbf{r} \quad (4.1)$$

where $G_\ell(\mathbf{r})$ is a convolution kernel, $\int_V G_\ell(\mathbf{r}) d^3 \mathbf{r} = 1$. Here we use a filter $G_\ell(\mathbf{r}) = \ell^{-3} \mathcal{G}(\mathbf{r}/\ell)$ based on the kernel $\mathcal{G}(\mathbf{r})$ which has the following Fourier transform

$$\hat{\mathcal{G}}(\mathbf{k}) \propto \begin{cases} \exp\left(-\frac{k^2}{1/4-k^2}\right) & k < 1/2 \\ 0 & k \geq 1/2 \end{cases} \quad (4.2)$$

where $k = |\mathbf{k}|$ (see Eyink & Aluie 2009, for details).

To include the density variations one also defines, for each field $a(\mathbf{x})$, a density-weighted (Favre) filtered field

$$\tilde{a}_\ell(\mathbf{x}) = \frac{\bar{\rho} a_\ell(\mathbf{x})}{\bar{\rho}_\ell(\mathbf{x})}. \quad (4.3)$$

By applying the filtering to Equations (2.1,2.2) one gets

$$\frac{\partial \bar{\rho}_\ell}{\partial t} + \nabla \cdot (\bar{\rho}_\ell \tilde{\mathbf{u}}_\ell) = 0, \quad (4.4)$$

$$\frac{\partial (\bar{\rho}_\ell \tilde{\mathbf{u}}_\ell)}{\partial t} + \nabla \cdot (\bar{\rho}_\ell \tilde{\mathbf{u}}_\ell \tilde{\mathbf{u}}_\ell) = -\nabla \cdot [\bar{\rho}_\ell (\tilde{\mathbf{u}} \tilde{\mathbf{u}}_\ell - \tilde{\mathbf{u}}_\ell \tilde{\mathbf{u}}_\ell)] - \nabla \bar{p}_\ell + \nabla \cdot \bar{\boldsymbol{\tau}}_\ell. \quad (4.5)$$

One can derive a filtered energy budget to get the following spatial averaged energy conservation equation (assuming a closed system) that removes the energy spatial transport

$$\frac{\partial \langle \mathcal{E}_\ell \rangle}{\partial t} + \langle \Pi_\ell + \Lambda_\ell - \bar{p}_\ell \nabla \cdot \tilde{\mathbf{u}}_\ell + D_\ell \rangle = 0 \quad (4.6)$$

where $\langle \cdot \rangle$ denotes spatial averaging ($\langle a(\mathbf{x}) \rangle = \int_V a(\mathbf{x}) d^3 \mathbf{x} / V$) and

$$\mathcal{E}_\ell = \frac{1}{2} \bar{\rho}_\ell |\tilde{\mathbf{u}}_\ell|^2, \quad (4.7)$$

$$\Pi_\ell = -\bar{\rho}_\ell \nabla \tilde{\mathbf{u}}_\ell : (\tilde{\mathbf{u}} \tilde{\mathbf{u}}_\ell - \tilde{\mathbf{u}}_\ell \tilde{\mathbf{u}}_\ell), \quad (4.8)$$

$$\Lambda_\ell = (\tilde{\mathbf{u}}_\ell - \bar{\mathbf{u}}_\ell) \cdot \nabla \bar{p}_\ell, \quad (4.9)$$

$$D_\ell = \nabla \tilde{\mathbf{u}}_\ell : \bar{\boldsymbol{\tau}}_\ell. \quad (4.10)$$

Equation (4.6) represents a coarse-graining equivalent to the KHM equation (3.6); $\partial\mathcal{E}_\ell/\partial t$ describes the (scale-dependent) kinetic energy decay, $\langle\Pi_\ell + \Lambda_\ell\rangle$ represents the energy transfer across scales, $\langle\bar{p}_\ell\nabla\cdot\bar{\mathbf{u}}_\ell\rangle$ is the (scale-dependent) pressure dilatation term, and $\langle D_\ell\rangle$ is the dissipation term. Similarly one can get the incompressible version of Equation (4.6) starting from Equation (3.1) (cf., Eyink & Aluie 2009) as

$$\frac{\partial\langle\mathcal{E}_\ell^{(i)}\rangle}{\partial t} + \langle\Pi_\ell^{(i)} + D_\ell^{(i)}\rangle = 0, \quad (4.11)$$

where

$$\mathcal{E}_\ell^{(i)} = \frac{1}{2}\rho_0|\bar{\mathbf{u}}_\ell|^2, \quad (4.12)$$

$$\Pi_\ell^{(i)} = -\rho_0\nabla\bar{\mathbf{u}}_\ell : (\bar{\mathbf{u}}\bar{\mathbf{u}}_\ell - \bar{\mathbf{u}}_\ell\bar{\mathbf{u}}_\ell), \quad (4.13)$$

$$D_\ell^{(i)} = \mu\nabla\bar{\mathbf{u}}_\ell : \nabla\bar{\mathbf{u}}_\ell, \quad (4.14)$$

and ρ_0 is the background density.

To test the validity of Equation (4.6), we define the departure from zero as

$$O_\ell = -\frac{\partial\langle\mathcal{E}_\ell\rangle}{\partial t} - \langle\Pi_\ell + \Lambda_\ell - \bar{p}_\ell\nabla\cdot\bar{\mathbf{u}}_\ell + D_\ell\rangle. \quad (4.15)$$

Figure 4 displays the results of the simulation of section 2 (solid lines), O_ℓ (normalized to Q_μ) as a function of ℓ as well as the different contributions, the decaying term (blue) $-\partial\mathcal{E}_\ell/\partial t$, the energy transfer term (green) $\langle\Pi_\ell + \Lambda_\ell\rangle$, the large scale pressure dilatation term (orange) $\langle\bar{p}_\ell\nabla\cdot\bar{\mathbf{u}}_\ell\rangle$, and the dissipation term $\langle D_\ell\rangle$. As in the KHM approach the calculation is done for times 6.2 and 6.3 over a reduced box 512^3 . Equation (4.6) is in the simulation well satisfied, the departure O_ℓ is small, $|O_\ell|/Q_\mu \sim 10^{-2}$.

Figure 4 shows, similarly to the KHM results, the decay, dissipation and pressure dilation terms go to zero on small scales and on large scales they reach their unfiltered counterparts: $\langle D_\ell\rangle \rightarrow Q_\mu$, $\partial\mathcal{E}_\ell/\partial t \rightarrow \partial\langle\rho|\mathbf{u}|^2\rangle/\partial t/2$, and $\langle\bar{p}_\ell\nabla\cdot\bar{\mathbf{u}}_\ell\rangle \rightarrow p\nabla\cdot\mathbf{u}$. The behaviors of the decay and dissipation terms are similar to their KHM counterparts (see Figure 3) but the characteristic scales differ. The pressure dilatation term is small but nonnegligible on all scales and overall decreases from large to small scales; this is also in agreement with the KHM results. The energy transfer (cascade rate) $\langle\Pi_\ell + \Lambda_\ell\rangle$ is important on medium scales and reaches a value comparable to that of the KHM cascade rate $-(\nabla_\ell\cdot\mathbf{Y} + R)/4$, about $0.7Q_\mu$; the main difference between the coarse graining and KHM results is the sign due to the different formulation of the scale-dependent energy conservation. A question is how the situation looks like for large Reynolds numbers where there may be an inertial range. The present results suggest that in this case the cascade rate will be compensated by the (constant) decay term in the inertial range

$$\langle\Pi_\ell + \Lambda_\ell\rangle = -\frac{1}{2}\frac{\partial\langle\rho|\mathbf{u}|^2\rangle}{\partial t}. \quad (4.16)$$

Figure 4 also shows (dashed lines) the results of the incompressible equivalent (see Equation (4.11))

$$O_\ell^{(i)} = -\frac{\partial\langle\mathcal{E}_\ell^{(i)}\rangle}{\partial t} - \langle\Pi_\ell^{(i)} + D_\ell^{(i)}\rangle. \quad (4.17)$$

As in the KHM case, the incompressible decay and dissipation terms are close to their compressible equivalents. The incompressible cascade rate $\langle\Pi_\ell^{(i)}\rangle$ is similar to that obtained for the incompressible KHM cascade. This supports the interpretation of R as an additional compressible cascade in the KHM equation.

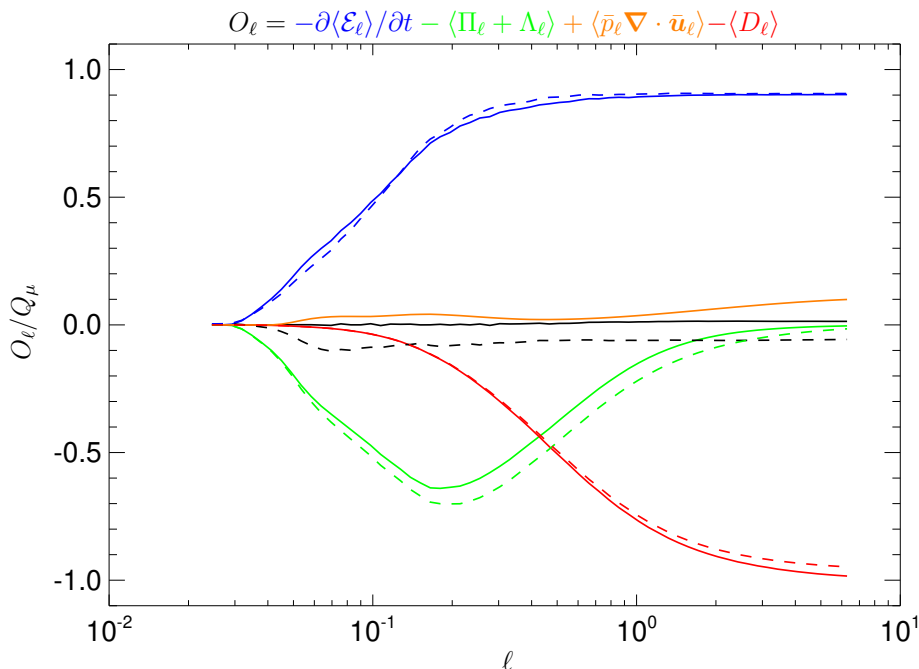


FIGURE 4. (solid) Departures from coarse-grained energy conservation (black) O_ℓ (given by Equation (4.15)) as a function of the filtering scale ℓ , along with the different contributions: the decaying term (blue) $-\partial \mathcal{E}_\ell / \partial t$, the energy transfer term (green) $\langle \Pi_\ell + \Lambda_\ell \rangle$, the pressure dilatation term (orange) $\langle \bar{p}_\ell \nabla \cdot \bar{\mathbf{u}}_\ell \rangle$, and the dissipation term $\langle D_\ell \rangle$. Dashed lines give the incompressible equivalents (black) $O_\ell^{(i)}$ (given by Equation (4.17)), along with the different contributions, the decaying term (blue) $-\partial \mathcal{E}_\ell^{(i)} / \partial t$, the energy transfer term (green) $\langle \Pi_\ell^{(i)} \rangle$, and the dissipation term $\langle D_\ell^{(i)} \rangle$. O_ℓ , $O_\ell^{(i)}$ and all their contributions are normalized to Q_μ .

5. Discussion

In this paper we investigated on the existence of the conservative cascade (inertial range) of the kinetic energy in compressible hydrodynamic turbulence. We compared the Kármán-Howarth-Monin and coarse-grained energy conservation approaches (in compressible and incompressible forms) for the kinetic energy, using data from a 3D HD decaying turbulence simulation with a moderate Reynolds number and the initial Mach number $M = 1$. In this simulation the two scale-dependent energy conservation equations are well satisfied. The pressure dilation coupling between the kinetic and internal energies are the strongest on large spatial scales and decrease towards smaller scales, in agreement with the results of Aluie *et al.* (2012). Coherently with the PSD of the kinetic energy which does not show a Kolmogorov spectrum, we do not observe a region where the kinetic-energy cascade dominates, the effects of decaying, pressure dilation and dissipation being not negligible. The KHM and coarse-graining approaches give rates of the cascade, decay, dissipation, and the pressure dilation processes that are in semi-quantitative agreement; the localization of these different processes is, however, different when expressed in the scale separation or filtering spatial scales. This is not surprising, calculations of structure functions and low-pass filtering are very different procedures. The kinetic energy decay and dissipation rates estimated from the incompressible approximations are close to the compressible predictions. In the simulation

the observed kinetic-energy cascade is weaker than that predicted by the incompressible KHM equation, showing that the compressible term R is not negligible.

In both approaches the pressure dilation terms $2\langle\delta p\delta\theta\rangle + C_p$ and $\langle\bar{p}_\ell\nabla\cdot\bar{\mathbf{u}}_\ell\rangle$ seem to be weak in the region where the kinetic energy cascade term dominates: We then expect that, depending on the level of compressibility, for a large enough Reynolds number (cf., Ishihara *et al.* 2009) an inertial range for the kinetic energy may exist. The pressure dilation effects typically weaken from large to small scales (Aluie *et al.* 2012) and also inclusion of forcing extends the region where the cascade dominates. The KHM and coarse-graining approaches could be used to determine the heating/cascade rate. The compressible equivalents of the incompressible “exact” laws, Equations (3.10) and 4.16, have different meanings, the KHM approach gives the (viscous) heating rate whereas the coarse graining approach relates to the kinetic-energy decay rate (or to the energy injection rate in the forced turbulence, cf., Aluie 2013).

In both the KHM and coarse-graining approaches only the cascade of kinetic energy is investigated. The effect of including also the isothermal internal energy as used by Galtier & Banerjee (2011) is questionable; the structure function $\langle\delta\rho\delta e\rangle$ proposed there does not represent well the internal energy (see appendix B). It is also questionable if a conservative cascade of the kinetic energy exists for strongly compressible (high Mach number) turbulence (Eyink & Drivas 2018; Drivas & Eyink 2018); an extension of this work to more compressible cases and/or larger Reynolds numbers is needed. The KHM structure function as well as coarse graining approaches may be further extended to (Hall) magnetohydrodynamics (MHD) (Yang *et al.* 2017; Andrés *et al.* 2018; Camporeale *et al.* 2018; Hellinger *et al.* 2018; Ferrand *et al.* 2019) and even combined (Eyink 2003; Kuzzay *et al.* 2019) to look at the localization of energy transfer processes. One limitation of the usual coarse-graining approach is that the filter is assumed to be isotropic; in anisotropic cases (such as in rotating HD or magnetized MHD) an anisotropic filter may be more appropriate; the KHM approach resolves this anisotropy rather naturally (Verdini *et al.* 2015).

Appendix A. Compressible Kármán-Howarth-Monin equation

Following Galtier & Banerjee (2011) we investigate the structure function $S = \langle\delta\mathbf{u}\cdot\delta(\rho\mathbf{u})\rangle$. To calculate $\partial S/\partial t$, we take Equation (2.2) at two different points, \mathbf{x}' and \mathbf{x} , and subtract them

$$\frac{\partial\delta\mathbf{u}}{\partial t} + (\mathbf{u}'\cdot\nabla')\mathbf{u}' - (\mathbf{u}\cdot\nabla)\mathbf{u} = -\frac{\nabla'p'}{\rho'} + \frac{\nabla p}{\rho} + \frac{1}{\rho'}\nabla'\cdot\boldsymbol{\tau}' - \frac{1}{\rho}\nabla\cdot\boldsymbol{\tau}. \quad (\text{A } 1)$$

Here the primed variables are those at \mathbf{x}' (including $\nabla' = \nabla_{\mathbf{x}'}$). Similarly from a modified version of Equation (2.2) we get

$$\frac{\partial\delta(\rho\mathbf{u})}{\partial t} + \mathbf{u}'\cdot\nabla'(\rho'\mathbf{u}') - \mathbf{u}\cdot\nabla(\rho\mathbf{u}) = -(\rho'\mathbf{u}')\nabla'\cdot\mathbf{u}' + (\rho\mathbf{u})\nabla\cdot\mathbf{u} - \nabla'p' + \nabla p + \nabla'\cdot\boldsymbol{\tau}' - \nabla\cdot\boldsymbol{\tau} \quad (\text{A } 2)$$

Taking $\delta(\rho\mathbf{u})$ times Equation (A 1) plus $\delta\mathbf{u}$ times Equation (A 2) after some manipulation we have

$$\begin{aligned} \frac{\partial S}{\partial t} + \nabla_{\mathbf{l}} \cdot \langle \delta\mathbf{u} [\delta(\rho\mathbf{u}) \cdot \delta\mathbf{u}] \rangle &= - \langle (\nabla' + \nabla) \cdot [\mathbf{u}\delta(\rho\mathbf{u}) \cdot \delta\mathbf{u}] \rangle \\ &\quad + \langle \rho' \mathbf{u}' \cdot \delta\mathbf{u} (\nabla \cdot \mathbf{u}) \rangle - \langle \delta\mathbf{u} \cdot (\rho\mathbf{u}) (\nabla' \cdot \mathbf{u}') \rangle \\ &\quad - \langle \delta\mathbf{u} \cdot \delta(\nabla p) \rangle - \left\langle \delta(\rho\mathbf{u}) \cdot \delta \left(\frac{\nabla p}{\rho} \right) \right\rangle \\ &\quad + \langle \delta\mathbf{u} \cdot \delta(\nabla \cdot \boldsymbol{\tau}) \rangle + \left\langle \delta(\rho\mathbf{u}) \cdot \left(\frac{\nabla \cdot \boldsymbol{\tau}}{\rho} \right) \right\rangle \end{aligned} \quad (\text{A } 3)$$

The first term at the right hand side disappears in the homogeneous approximation and after some manipulation one gets Equation (3.6).

Appendix B. Internal Energy

Galtier & Banerjee (2011) investigated the KHM equation for the total energy by representing the internal energy by the structure function

$$S_e = \langle \delta\rho\delta e \rangle \quad (\text{B } 1)$$

where e is the internal energy density. It is interesting to look at the properties of S_e in the simulation of section 2. For e , in our case $e = T/(\gamma - 1)$, one gets the following relation from Equation (2.3)

$$\frac{\partial e}{\partial t} + (\mathbf{u} \cdot \nabla)e = \alpha\Delta e - \frac{1}{\rho}p\theta + \frac{1}{\rho}\boldsymbol{\tau} : \boldsymbol{\Sigma}. \quad (\text{B } 2)$$

Using the same approach as in appendix A one gets the following KHM-like equation

$$\frac{\partial S_e}{\partial t} + \nabla_{\mathbf{l}} \cdot \mathbf{Y}_e + R_e = \alpha \langle \delta\rho\delta(\Delta e) \rangle - \mathcal{D}(p\theta) + \mathcal{D}(\boldsymbol{\tau} : \boldsymbol{\Sigma}), \quad (\text{B } 3)$$

where

$$\mathbf{Y}_e = \langle \delta\mathbf{u}\delta\rho\delta e \rangle, \quad (\text{B } 4)$$

$$R_e = \langle \delta e \rho \nabla' \cdot \mathbf{u}' - \rho' \delta e \nabla \cdot \mathbf{u} \rangle, \quad (\text{B } 5)$$

and

$$\mathcal{D}(a) = \left\langle \left(1 - \frac{\rho}{\rho'} \right) a' + \left(1 - \frac{\rho'}{\rho} \right) a \right\rangle \quad (\text{B } 6)$$

In Equation (B 3) $\nabla_{\mathbf{l}} \cdot \mathbf{Y}_e + R_e$ represents the energy transfer connected with S_e . The r.h.s of Equation (B 3) strongly depends on the density variation; for a constant ρ this side is zero. Combining Equation (3.6) with Equation (B 3) as $\partial(S/2 + S_e)/\partial t$ one recovers to a large extent the results of Galtier & Banerjee (2011), except for the isothermal closure (and the forcing term); pressure-dilation effects are in Galtier & Banerjee (2011) transformed to a contribution to the cascade term using the isothermal closure

To test Equation (B 3) on the simulation results of section 2, we define the departure (see section 3) as

$$O_e = \frac{1}{2} \left[-\frac{\partial S_e}{\partial t} - \nabla_{\mathbf{l}} \cdot \mathbf{Y}_e - R_e + \alpha \langle \delta\rho\delta(\Delta e) \rangle - \mathcal{D}(p\theta) + \mathcal{D}(\boldsymbol{\tau} : \boldsymbol{\Sigma}) \right]. \quad (\text{B } 7)$$

Figure 5 shows the (isotropized) departure (black) O_e as a function of the scale l along

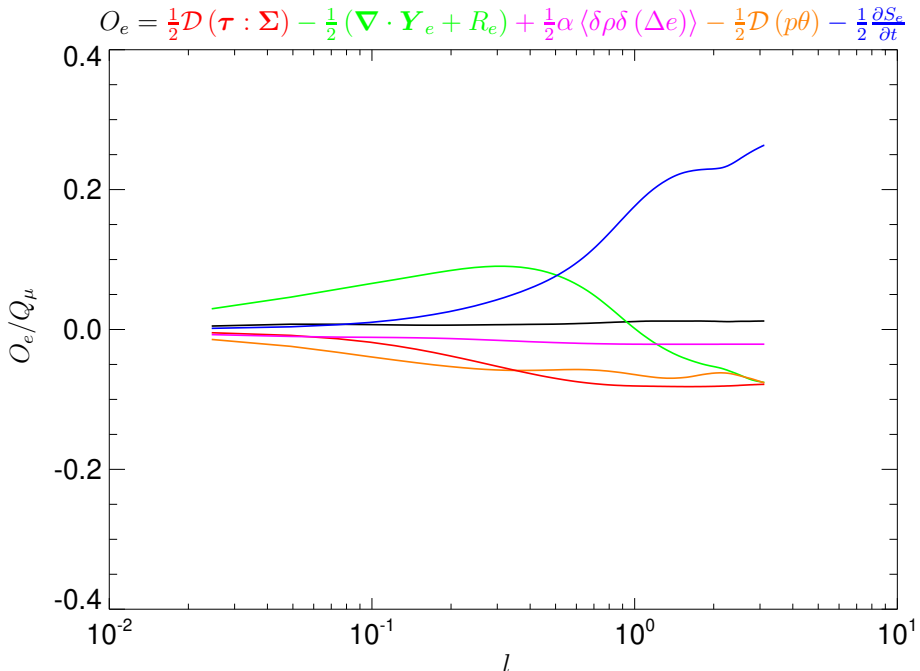


FIGURE 5. (black) The departure O_e (given by Equation (B7)) as a function of the scale l along with the different contributions, the decaying term (blue) $-\partial S_e/\partial t/2$, the energy transfer term (green) $-(\nabla_l \cdot \mathbf{Y}_e + R_e)/2$, the pressure dilatation term (orange) $-\mathcal{D}(p\theta)/2$, and (red) the dissipation term $\mathcal{D}(\boldsymbol{\tau} : \boldsymbol{\Sigma})$, and the diffusion term (magenta) $\alpha \langle \delta\rho\delta(\Delta e) \rangle$. O_e and all its contributions are normalized to Q_μ .

with the different contributions, the decaying term (blue) $-\partial S_e/\partial t/2$, the energy transfer term (green) $-(\nabla_l \cdot \mathbf{Y}_e + R_e)/2$, the pressure dilatation term (orange) $-\mathcal{D}(p\theta)/2$, and (red) the dissipation term $\mathcal{D}(\boldsymbol{\tau} : \boldsymbol{\Sigma})$, and the diffusion term (magenta) $\alpha \langle \delta\rho\delta(\Delta e) \rangle$. The calculation is done on a sub-grid of 256^3 points taking every fourth point in all directions. Figure 5 confirms that the energy-like conservation, Equation (B3), is well satisfied, $|O_e|/Q_\mu \sim 1\%$ and shows that all the terms are nonnegligible, including the diffusion.

One important thing to note from Figure 5 is that $\partial S_e/\partial t < 0$. The structure function $S_e = \langle \delta\rho\delta e \rangle$ decreases with the time in contrast with the internal energy $E_i = \langle \rho e \rangle$ that increases (see Figure 1). If S and S_e are to represent kinetic and internal energy, respectively, in an analogous way, the latter should increase as the former decreases. This is a clear indication that S_e does not well represent the internal energy. Consequently, the terms $\nabla_l \cdot \mathbf{Y}_e + R_e$ are not clearly related to a cascade/energy transfer of the internal energy.

P.H. acknowledges grant 18-08861S of the Czech Science Foundation.

Declaration of Interests. The authors report no conflict of interest.

REFERENCES

- ALUIE, H. 2011 Compressible turbulence: The cascade and its locality. *Phys. Rev. Lett.* **106**, 174502.
- ALUIE, H. 2013 Scale decomposition in compressible turbulence. *Physica D* **247**, 54–65.
- ALUIE, H., LI, S. & LI, H. 2012 Conservative cascade of kinetic energy in compressible turbulence. *Astrophys. J. Lett.* **751**, L29.

- ANDRÉS, N., GALTIER, S. & SAHRAOUI, F. 2018 Exact law for homogeneous compressible hall magnetohydrodynamics turbulence. *Phys. Rev. E* **97**, 013204.
- CAMPOREALE, E., SORRISO-VALVO, L., CALIFANO, F. & RETINÒ, A. 2018 Coherent structures and spectral energy transfer in turbulent plasma: A space-filter approach. *Phys. Rev. Lett.* **120**, 125101.
- DE KARMAN, T. & HOWARTH, L. 1938 On the statistical theory of isotropic turbulence. *Proc. Royal Soc. London Series A* **164**, 192–215.
- DRIVAS, T. D. & EYINK, G. L. 2018 An onsager singularity theorem for turbulent solutions of compressible Euler equations. *Commun. Math. Phys.* **359**, 733–763.
- EYINK, G. L. 2003 Local 4/5-law and energy dissipation anomaly in turbulence. *Nonlinearity* **16**, 137–145.
- EYINK, G. L. & ALUIE, H. 2009 Localness of energy cascade in hydrodynamic turbulence. I. Smooth coarse graining. *Phys. Fluids* **21**, 115107.
- EYINK, G. L. & DRIVAS, T. D. 2018 Cascades and dissipative anomalies in compressible fluid turbulence. *Phys. Rev. X* **8**, 011022.
- FERRAND, R., GALTIER, S., SAHRAOUI, F., MEYRAND, R., ANDRÉS, N. & BANERJEE, S. 2019 On exact laws in incompressible Hall magnetohydrodynamic turbulence. *Astrophys. J.* **881**, 50.
- FRIGO, M. & JOHNSON, S. G. 2005 The design and implementation of FFTW3. *Proc. IEEE* **93**, 216–231.
- FRISCH, U. 1995 *Turbulence*. Cambridge University Press.
- GALTIER, S. & BANERJEE, S. 2011 Exact relation for correlation functions in compressible isothermal turbulence. *Phys. Rev. Lett.* **107**, 134501.
- GERMANO, M. 1992 Turbulence: The filtering approach. *J. Fluid Mech.* **238**, 325–336.
- GOTOH, T., FUKAYAMA, D. & NAKANO, T. 2002 Velocity field statistics in homogeneous steady turbulence obtained using a high-resolution direct numerical simulation. *Phys. Fluids* **14**, 1065–1081.
- HELLINGER, P., VERDINI, A., LANDI, S., FRANCI, L. & MATTEINI, L. 2018 von Kármán-Howarth equation for Hall magnetohydrodynamics: Hybrid simulations. *Astrophys. J. Lett.* **857**, L19.
- ISHIHARA, T., GOTOH, T. & KANEDA, Y. 2009 Study of high-Reynolds number isotropic turbulence by direct numerical simulation. *Annu. Rev. Fluid Mech.* **41**, 165–180.
- KOLMOGOROV, A. N. 1941 Dissipation of energy in locally isotropic turbulence. *Akademiia Nauk SSSR Doklady* **32**, 16.
- KUZZAY, D., OLGA, A. & MATTEINI, L. 2019 Local approach to the study of energy transfers in incompressible magnetohydrodynamic turbulence. *Phys. Rev. E* **99**, 053202.
- MONIN, A. S. & YAGLOM, A. M. 1975 *Statistical fluid mechanics: Mechanics of turbulence*. Cambridge, MA, USA: MIT Press.
- PEKUROVSKY, D. 2012 P3DFFT: a framework for parallel computations of Fourier transforms in three dimensions. *SIAM J. Sci. Comput.* **34**, C192–C209.
- VERDINI, A., GRAPPIN, R., HELLINGER, P., LANDI, S. & MÜLLER, W. C. 2015 Anisotropy of third-order structure functions in MHD turbulence. *Astrophys. J.* **804**, 119.
- YANG, Y., MATTHAEUS, W. H., SHI, Y., WAN, M. & CHEN, S. 2017 Compressibility effect on coherent structures, energy transfer, and scaling in magnetohydrodynamic turbulence. *Phys. Fluids* **29**, 035105.